We are IntechOpen,
the world's leading publisher of
Open Access books
Built by scientists, for scientists

4,800
Open access books available

122,000
International authors and editors

135M
Downloads

Our authors are among the

154
Countries delivered to

TOP 1%
most cited scientists

12.2%
Contributors from top 500 universities

Selection of our books indexed in the Book Citation Index
in Web of Science™ Core Collection (BKCI)

Interested in publishing with us?
Contact book.department@intechopen.com

Numbers displayed above are based on latest data collected.
For more information visit www.intechopen.com

Nanostructured Metal Oxides-Based Electrode in Supercapacitor Applications

Zhenjun Qi, Shihao Huang, Adnan Younis,
Dewei Chu and Sean Li

Additional information is available at the end of the chapter

Abstract

To overcome the obstacle of low energy density, one of the most intensive approaches is the development of new materials for supercapacitor electrodes. Most explored materials today are carbon particle materials, which have high surface areas for charge storage. But in spite of these large specific surface areas, the charges physically stored on the carbon particles in porous electrode layers are unfortunately limited. Regarding advanced supercapacitor electrodes, metal oxides are considered the most promising material for the next generation of supercapacitors owing to their unique physical and chemical properties. In this chapter, the rational design and fabrication of metal oxide nanostructures for supercapacitor applications are addressed.

Keywords: supercapacitor, metal oxide, nanostructure, nanocomposite, graphene

1. Introduction

In recent years, supercapacitors (or ultracapacitors) have attracted significant attention as a versatile solution to meet the increasing demands of energy storage because of their fast power energy delivery, long lifecycle, high power density and reasonably high energy density which are able to fill in the gap between the batteries and the conventional capacitors [1–3].

The comparison of specific power and specific energy for different electrical energy storage devices is shown in the Ragone plot (**Figure 1**) [4]. The data illustrate that supercapacitors are able to store more energy than conventional capacitors and deliver more power than batteries. Owing to the different energy storage mechanism from conventional capacitors, the specific

INTECH
open science | open minds

energy of supercapacitors can be thousands of times higher than it of conventional capacitors by forming an electric double layer at the interface of the electrode and electrolyte to store energy [5]. Thus, the high surface area of the electrode can be adequately utilized to collect amounts of positively and negatively charged ions from electrolyte when storing energy.
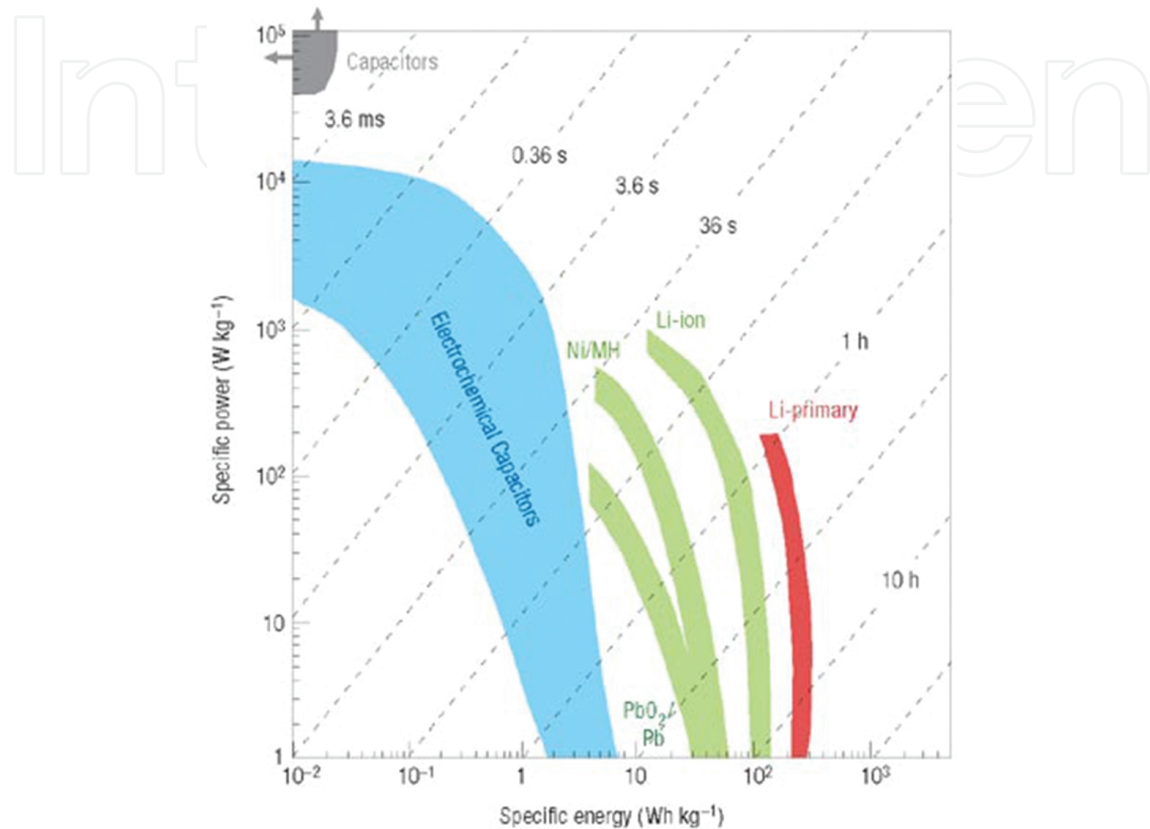

Figure 1. Specific power and energy for various electrical energy storage devices show in Ragone plot [4].

On the other hand, as is well-known, rechargeable batteries mainly depend on chemical reactions to charge and discharge which significantly restrict their lifetime [6]. Compared to batteries, the energy storage process of supercapacitors is based on electrostatic storage in the electrical double layer and reversible faradaic redox reactions by means of electron charge transfer on the surface of electrode. Thus, supercapacitors are expected to have a capability of faster charge–discharge under high current and a longer cycle life than batteries because no or negligibly few chemical reactions are involved [7].

Even though major progress has been yielded in the theoretical and practical research and development of supercapacitors, few disadvantages of supercapacitors, including low energy density and high production cost, have been identified as major challenges for the furtherance of supercapacitors technologies [8].

To overcome the obstacle of low energy density, one of the most intensive approaches is the development of new materials for supercapacitor electrodes. Most explored materials today are carbon particle-based materials, which have high surface areas for charge storage [3]. But

in spite of these large specific surface areas, the charges physically stored on the carbon particles in porous electrode layers unfortunately limiting their electrochemical properties. Supercapacitors of this kind, called electrical double-layer supercapacitors (EDLS), have a limited specific capacitance and relative low energy density [9]. Supercapacitors with electro-chemically active materials (polymers and metal oxides) as electrodes involving fast and reversible faradaic reactions on electrodes are called faradaic supercapacitors (FS). It has been demonstrated that faradaic or hybrid double-layer supercapacitors can yield much higher specific capacitance and energy density. Thus, regarding advanced supercapacitor materials, metal oxides are considered the most promising materials for the next generation of superca-pacitors [10].
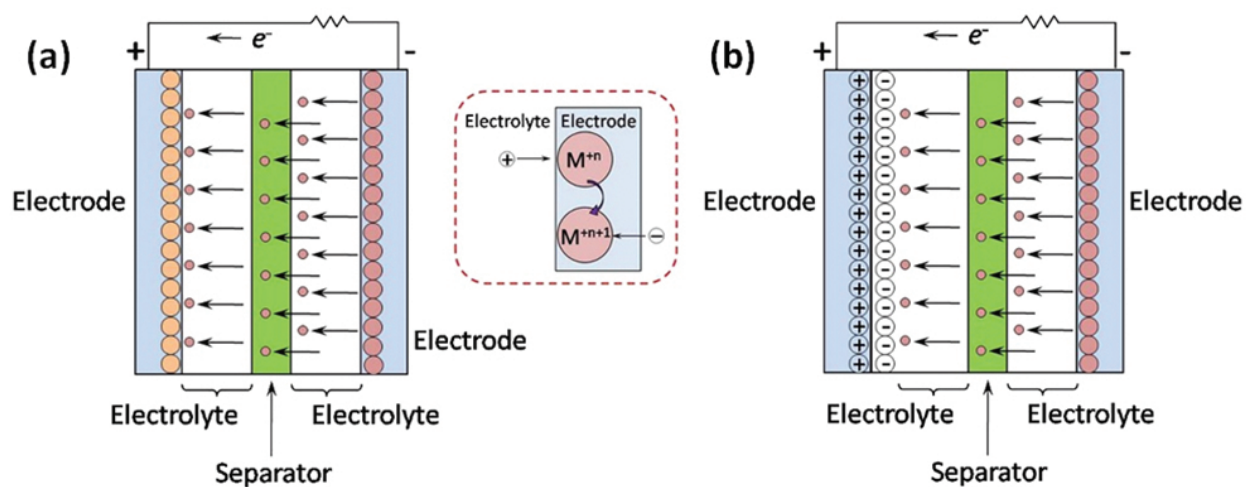

Figure 2. Mechanisms of (a) pseudocapacitance and (b) hybrid capacitance [13].

The capacitance of a metal oxide-based supercapacitor is determined by two storage principles, one is double-layer capacitance and another one is pseudocapacitance. The mechanism of double-layer capacitance is shown in **Figure 2a**, when capacitor charged, electrostatic storage achieved by separation of charge in a double layer at the interface between the surface of a conductive electrode and an electrolyte. As a result, mirror image of charge distribution of ions in opposite polarity, called double-layer, is formed. When capacitor discharged, ions return and distribute randomly in the electrolyte. For pseudocapacitance, it stores electrical energy electrochemically by means of reversible faradaic redox reactions on the surface of suitable electrode materials in an electrochemical capacitor with an electric double-layer [11]. It can be seen in **Figure 2b**, pseudocapacitance is accompanied with an electron charge-transfer between electrolyte and electrode coming from a de-solvated and adsorbed ion whereby only one electron per charge unit is participating. This faradaic charge transfer originates via a very fast sequence of reversible redox, electrosorption or intercalation processes. The adsorbed ion has no chemical reaction with the atoms of the electrode. No chemical bonds arise, and only a charge-transfer takes place [12]. Even though both double-layer capacitance and pseudocapa-citance contribute indivisibly to the total capacitance of metal oxide supercapacitors, the latter can be 10–100 times higher than the former.

In general, metal oxide-based supercapacitors are able to possess higher specific capacitance and energy density than carbon materials and conducting polymer materials [14]. A series of metal oxides with high theoretical performances has been studied, such as RuO_2, MnO_2, NiO, Co_3O_4, V_2O_5, CuO and Fe_3O_4. **Table 1** [15] lists the theoretical capacitance of some typical metal oxides as well as the charge storage reactions. However, the practical supercpacitive properties of these metal oxides are far behind their theoretical values due to their low conductivities, poor long-term stability, low surface areas and porosity.

Oxide	Electrolyte	Charge storage reaction	Theoretical capacitance (F g^{-1})	Conductivity (S cm^{-1})
MnO_2	Na_2SO_4	$MnO_2 + M^+ + e^- = MMnO_2$ (M could be H^+, Li^+, Na^+, K^+)	1380	10^{-5} to 10^{-6}
V_2O_5	NaCl, Na_2SO_4	$V_2O_5 + 4M^+ + 4e^- = M_2V_2O_5$ (M could be H^+, Li^+, Na^+, K^+)	2120	10^{-4} to 10^{-2}
NiO	KOH, NaOH	$NiO + OH^- = NiOOH + e^-$	2584	0.01 to 0.32
Co_3O_4	KOH, NaOH	$Co_3O_4 + OH^- + H_2O = 3CoOOH + e^-$ $CoOOH + OH^- = CoO_2 + H_2O + e^-$	3560	10^{-4} to 10^{-2}

Table 1. Pseudocapacitance and conductivity of selected metal oxides.

In this chapter, several important factors affecting the electrochemical properties of metal oxide-based electrodes are discussed firstly. Then various methods to fabricate nanostructured metal oxide electrode are summarized. Finally, advanced metal oxide-carbon composite electrodes are further described.

2. Factors affecting the performance of metal oxide-based electrodes

2.1. Crystallinity

The degree of crystallinity is one of pivotal factors affecting the pseudocapacitance of metal oxide materials. In general, an amorphous structure exhibits superior electrochemical performance than a well-crystallized structure due to the former can make the fast, continuous and reversible faradaic reaction take place not only on the surface but also inside of metal oxide particles [16]. This is because the amorphous structure with a highly porous morphology is benefit for ion accessibility and cation diffusion. In addition, these porous structures also result in a higher specific surface area which can support more redox reactions to enhance the specific capacitance. Nevertheless, it is well-known that the poorly crystallized metal oxide simultaneously leads to a lower electrical conductivity limiting its pseudocapacitance. Thus, it is necessary and a great challenge to explore the appropriate crystallinity with optimal conductivity and ionic transport.

One method is to improve the electric conductivity of the amorphous metal oxide. It has been reported that annealing can significantly affect the electrical conductivity. For example, in [17], MnOx annealed at 200°C exhibited a higher specific capacitance at high scan rate than those without treated. Another effective approach is to optimize the structure of crystallized metal oxide in order to provide appropriate tunnels for the intercalation of cations.

2.2. Crystal structure

The crystal structure has a significant influence on the pseudocapacitance of metal oxide because it plays a crucial role in determining the cations intercalation. For instance, crystallized manganese oxide has different crystalline structures, including α-, β-, γ-, δ- and λ-MnO_2 shown in **Figure 3** [18]. It can be seen thatα-MnO_2 forms 1D (2×2) and (1×1) tunnels; β-MnO_2 forms a 1D (1×1) tunnel; γ-MnO_2 is consist of 1D (1×2) and (1×1) tunnels; δ-MnO_2 is a 2D layered structure; and λ-MnO_2 is a three-dimensional (3D) spinel structure, respectively [11, 19]. It is reported by Brousse et al. [20] that α-MnO_2 with a large tunnel size exhibited a relatively high specific capacitance of 110 F g^{-1} due to K^+ cations could easily insert the tunnels. On the contrary, β-MnO_2 with a narrow tunnel size which is smaller than K^+ cations inhibited the diffusion process and leaded to a low specific capaci-
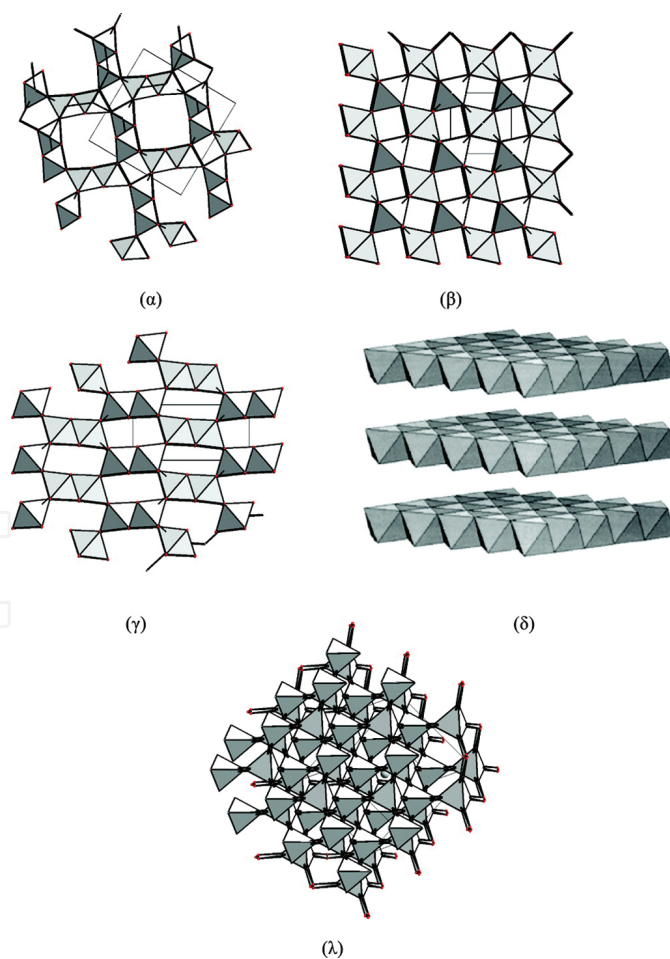

(α)   (β)

(γ)   (δ)

(λ)

Figure 3. Crystal structures of α-, β-, γ-, δ- and λ-MnO_2 [18].

tance value of only 110 μF cm^{-2}. The result indicated that the limited performance was manly obtained on the surface of manganese oxide. Furthermore, the 2D δ-MnO$_2$ with an interlayer separation of around 0.7 nm also obtained good capacitance value of 236 F g^{-1} which could be contributed to the sufficiently large layer space for a high rate insertion/extraction of K$^+$ cations.

Thus, the rational selection of crystal structures can effectively accelerate the charge storage process of metal oxide and improve its electrochemical properties.

2.3. Specific surface area

The pseuocapacitance of metal oxide depends on redox reactions which mainly take place on the surface area. Thus, the specific surface area is one of the most important factors for metal oxide-based supercapacitor applications. In general, the higher specific surface area can result in the higher the specific capacitance due to more active sites are capable of providing multiple redox reactions [21].

Obviously, to explore the higher specific surface area is an effective approach to achieve better capacitive performance of metal oxide. Up to now, amounts of attempts have been made on metal oxides including decreasing the size of their particles, optimizing their morphologies and combining them with carbon materials which have high specific surface areas.

2.4. Morphology

The morphology of metal oxide is a crucial factor which closely relates to the specific surface area, the diffusion pathway, surface to volume ratios and therefore the supercapacitive performance. Thus, considerable efforts have been focused on various metal oxides with different morphologies such as nanowires, nanorods, nanotubes, nanoflowers, hollow spheres, nanopillar array and porous thin films.

Several morphologies of metal oxide and their supercapacitive performance are discussed in this part. The first morphology is one-dimensional nanostructured metal oxides which generally enhance the specific capacitance through offering short diffusion path lengths for both ions and electrons as well as a large specific surface area. Gao et al. [22] successfully synthesized Co$_3$O$_4$ nanowires on nickel foam via template-free method shown in **Figure 4a**. The nanowires, with diameters around 250 nm and the lengths up to around 15 μm, displayed a maximum specific capacitance of 746 F g^{-1} at a current density of 5 mA cm^{-2}. In addition, Lu et al. [23] reported a slim (<20 nm) NiO nanorod structure (**Figure 4b**) had an ultrahigh specific capacitance of 2018 F g^{-1} (80% of the theoretical value) at a current density of 2.27 A g^{-1} and high power density of 1536 F g^{-1} at 22.7 A g^{-1}. Generally, the diameter plays an important role in one-dimensional nanostructure. The smaller diameter can offer larger specific surface area and more active sites leading to a better specific capacitance. It is also reported that the porous nanotube structure of MnO$_2$ could not only enhance the specific capacitance, but also improve the stability of electrode due to accommodating large volume charges during the charge-discharge cycle [24]. The second metal oxide structure should be noted is hollow spheres. Various metal oxides with hollow sphere morphologies

have been successfully synthesized recently to pursue a high loosely mesoporous structure, large specific surface area and fast ion/electron transfer. For example, Yan et al. [25] fabricated hierarchically porous NiO hollow spheres composed of nanoflakes shown in **Figure 4c** with thicknesses of ~10 nm via a powerful chemical bath deposition method. The specific capacitance of NiO hollow spheres can remain 346 F g^{-1} at 1 A g^{-1} after 2000 cycles indicating an excellent supercapacitive performance. Another example is [26] that Co_3O_4 hollow spheres prepared by a facile carbonaceous microsphere templated synthesis as shown in **Figure 4d**. The as-obtained Co_3O_4 hollow spheres are composed of nanoparticles and possess a high surface area of 60 m^2 g^{-1} owing to their mesoporous structure. Such a unique hollow-sphere architecture can greatly contributed to the comparatively high capacitance and excellent cycling stability. The third type of metal oxide morphology is three-dimensional porous structure. It can be seen in **Figure 4e** that 3D highly ordered nanoporous CuO with interconnected bimodal nanopores were fabricated by Moosavifard and coworkers [27]. This morphology offered a large specific surface area of 149 m^2 g^{-1} displayed an excellent specific capacitance of 431 F g^{-1} at 3.5 mA cm^{-2} due to the 3D porous structure providing facilitated ion transport, short ion and electron diffusion pathways and more active sites for electrochemical reactions. Moreover, 3D-nanonet hollow structured Co_3O_4,
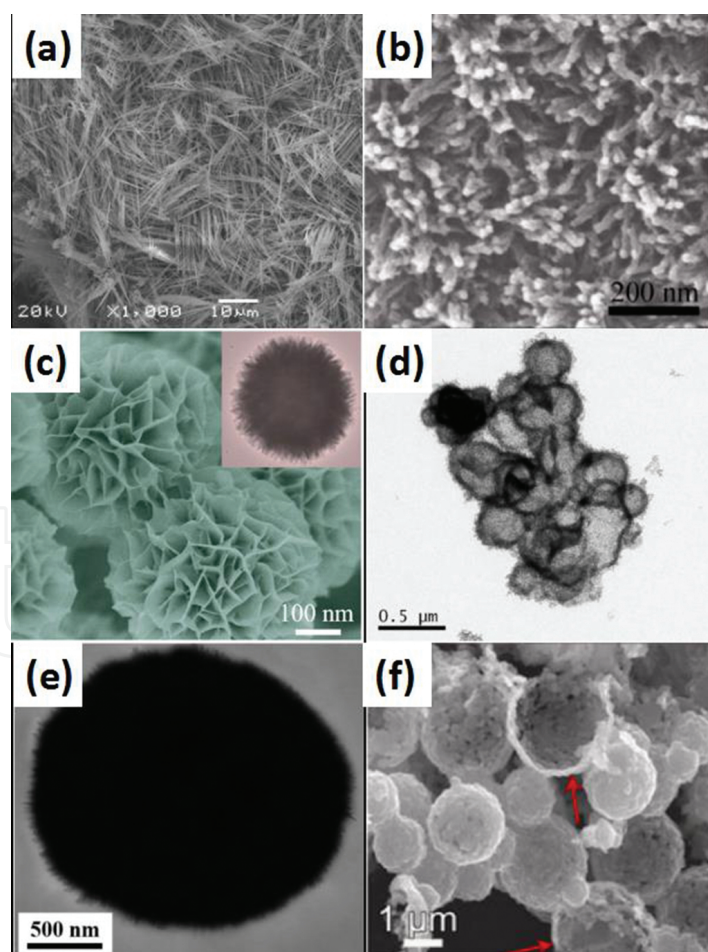

Figure 4. (a) Co_3O_4 nanowires [22]; (b) NiO nanorods [23]; (c) NiO hollow spheres [25]; (d) Co_3O_4 hollow spheres [26]; (e) 3D highly nanoporous CuO [27]; and (f) 3D nanonet hollow structured Co_3O_4 [28].

shown in **Figure 4f**, exhibited a maximum specific capacitance of 820 F g^{-1} at a scan rate of 5 mV s^{-1} and remained 90.2% of its initial capacitance after 1000 cycles [28]. The above results have proven that three-dimensional porous structured metal oxide is promising for supercapacitor applications.

As mentioned above, the electrochemical properties of metal oxide-based supercapacitors are largely affected by the morphologies. The rational design of morphologies with high specific surface area and porous nanostructures is necessary for the development of metal oxide-based electrodes.

2.5. Conductivity

It is well-known that the electronic conductivity of electrode materials is a vital factor to affect their high performance in supercapacitor applications. Unfortunately, the electronic conductivity of metal oxide materials is generally poor which largely limits ion and electron transfer. When the charge/discharge rate increases, the low conductivity would result in the localized charge/discharge process in a limited volume near the current collector, leading to low specific capacitance and low rate capability. For example, due to the low electronic conductivity ($\sim 10^{-5}$ to 10^{-6} S cm^{-1}), the realistic specific capacitance of manganese oxide is usually up to 350 F g^{-1} far behind its theoretic value of 1370 F g^{-1} [15, 29]. The same condition also takes place on other metal oxide materials such as NiO, Co_3O_4 and V_2O_5 [30, 31].

Thus, it is urgent to improve the conductivity of metal oxide in order to an ideal supercapacitive performance. One effective approach is doping metal elements into metal oxide and compositing metal oxide with high conductive carbon materials and conducting polymer.

2.6. Mass loading

The quantity of active materials loading on substrates can affect the specific capacitance, power and energy performance of metal oxide electrodes. On one hand, the large mass loading can cause longer transport paths for the diffusion of protons and an increase of thickness of metal oxide thin films resulting in lower electrical conductivity, limited access of electrolyte ions and higher series resistance. As a result, only partial active material on the surface of electrode film takes part in the charge storage leading to a lower specific capacitance of metal oxide. It is reported by Yang et al. [32] the specific capacitance of MnO_2 thin films decreased from 203 to 155 F g^{-1} when the mass loading increased from 6 to 18 mg cm^{-2}. On the other hand, a high mass loading is needed for high power and energy density, which thus makes the application of a light and durable supercapacitor possible [11]. Therefore, it is still a challenge for metal oxide to achieve both high mass loading and excellent specific capacitance.

3. Typical synthesis methods of metal oxide nanostructures

Nanostructured metal oxide materials have been intensively investigated due to their superior supercapacitive performance. The factors mentioned above are all related to the metal oxide

fabrication processes and parameters. The main synthesis techniques exploited include hydrothermal, electrodeposition, sol–gel, microwave assisted as well as template assisted methods.

3.1. Hydrothermal method

Hydrothermal synthesis is well-known as one of the most outstanding approaches to prepare nanoparticles due to a serious of advantages such as fine powder (nanoscale), high purity, good dispersion, uniform, narrow distribution, without agglomeration, good crystal form and shape controllability. In a hydrothermal process, crystal grows by chemical reactions taking place at high temperature and pressure conditions in a sealed pressure vessel with water as solvent. Under hydrothermal conditions, water can act as a chemical component and participate in the reactions. Moreover, the solvent is not only a mineralizing agent but also a pressure medium. By the control of physical and chemical factors, the formation and modification of nanostructured metal oxide can be achieved. Up to now, hydrothermal method has been successfully used to synthesize metal oxide with various nanostructures, such as nanowires, nanorods, nanoflowers, nanospheres, nanosheets, nanotubes and so on.

Purushothaman and his group [33] successfully prepared NiO nanoparticles via the hydrothermal method, using SDS as a surfactant. The different temperatures (120, 140, 160 and 180°C) in hydrothermal processes have been studied to optimize the morphology and electrochemical properties of NiO. The high degree of phase purity of the NiO particles with nanosizes of 8–16 nm have been achieved under all selected temperatures. However, the morphologies and electrochemical properties were different. At 120 and 140°C, the assembly of nanosheets is slow and, hence, they probably assemble into microspheres under the assistance of a surfactant. A decrease in the surface tension with increasing preparation temperature results in weak electrostatic interaction. The reduced surface tension lowers the aggregation, enabling the formation of microspheres with well-resolved nanosheets at 160°C. The initial nucleation and growth rate will be faster at 180°C. The faster nucleation hinders the assembly of anion surfactant and cation, resulting in the formation of nanorod assembled thicker plates. In case of supercapacitance, the sample prepared at 120°C exhibited a specific capacitance of 871 F g^{-1}, while the value of sample formed at 140°C was 925 F g^{-1}. The maximum specific capacitance of 989 F g^{-1} was obtained at 160°C while the specific capacitance showed a reduced value of 496 F g^{-1} at 180°C. The formation of a nanosheet-like structure seem to have facilitated the ion exchange process by reducing the diffusion lengths for the electrolyte, yielding a superior redox process in the sample prepared at 160°C, which exhibited the best specific capacitance. The specific capacitance was lower at elevated temperatures (180°C) might because the crystallites of larger size were formed, and they limited the paths available for ion transport. Moreover, Xia et al. [34] synthesized hollow Co$_3$O$_4$ nanowire arrays through a facile hydrothermal method. The Co$_3$O$_4$ nanowires have an average diameter of 200 nm, and the hollow centers have a diameter of 25 nm. In addition, a hierarchically porous can be found in nanowires allowing easier electrolyte penetration. Such a novel structure with porous walls and hollow center possesses more sites for ions to enter and allows facile ion diffusion at high

current density leading to superior specific capacitances of 599 F g^{-1} at a current density of 2 A g^{-1} and 439 F g^{-1} at 40 A g^{-1}.

3.2. Electrodeposition methods

Electrochemical deposition is a simple, fast, nonpolluting and facile technique, thus becomes one of most commonly used approaches to prepare metal oxide thin films. An electrochemical synthesis is achieved by a series of procedures that electron transfer between two or more electrodes separated by electrolyte making the occurrence of oxidation or reduction in the electrode–electrolyte interface which finally results in thin films deposited on electrode substrates. Electrochemical deposition can be divided into two different methods: anodic deposition and cathodic deposition. For example, Aghazadeh [35] prepared nanostructured Co$_3$O$_4$ via a simple cathodic electrodeposition method. The porous Co$_3$O$_4$ nanoplates displayed the average pore diameter and the surface area of 4.75 nm and 208.5 m^2 g^{-1}, respectively. A good specific capacitance as high as 393.6 F g^{-1} at the constant current density of 1 A g^{-1} and an excellent capacity retention (96.5% after 500 charge-discharge cycles) was obtained. Deng et al. [36] have reported that the nanoarchitectured CuO electrodes with a 3D hierarchically porous structure were prepared by an anodic electrodeposition method. An exceptionally large specific capacitance of 880 and 800 F g^{-1} was obtained at scan rates of 10 and 200 mV s^{-1}.

According to the different modes of external power supplying, three main electrochemical deposition techniques including potentiostatic, galvanostatic and pulse period methods have been used by researchers. These different deposition routes with different applied current, potential and time have a crucial impact on the surface morphologies and crystal structures of metal oxide thin films. For example, Lee et al. [37] electrodeposited manganese oxide using three different modes: constant potential (CP) at 1 V for 900 s, pulse potential (PP) at 1 and 0 V with 0.5 s/0.5 s on-off time for 10,000 s, and pulse reverse potential (PRP) at 1 V and −1 V with 0.5 s/0.5 s interval time for 10,000 s. The different deposition times are applied to obtain similar mass loading. The results demonstrated that the different electrodeposition methods have a significant influence on the morphologies of manganese oxide. A traditional bulk film composed of 100 nm particles was prepared by CP mode and exhibited relatively low specific capacitance of 184 F g^{-1} at a scan rate of 10 mV s^{-1}. In case of PP mode, nanostructured MnOx with porous flower petals morphology was obtained and showed a higher specific capacitance of 227.7 F g^{-1}. The highest specific capacitance of 448 F g^{-1} was achieved by PRP mode due to the formation of nanorods with the average diameter of 20 nm which can supply higher specific surface area and faster ion transfer.

3.3. Sol–gel method

The sol–gel technique also attracts significant attention for the synthesis of nanostructured metal oxides because it offers controllable purity, composition, homogeneity of the products. Kim et al. [38] have reported that NiO nanostructures with three distinct morphologies were fabricated by a sol–gel method. The nanoflower structure was created in hexamethylene tetramine (HMTA) solution, while the nanoslice (diameters of 300–530 nm) was prepared in ammonium hydroxide (NH$_4$OH) solution. The smaller nanoparticles with

a diameter of around 50 nm were obtained when the reaction process took place in a strong basic LiOH. In addition, their morphology-dependent supercapacitor properties were exploited. Compared to the nanoslice and nanoparticle-shaped NiO, the nanoflower-shaped NiO showed the best supercapacitor properties (480 F g^{-1} at 0.5 A g^{-1}) despite it having the lowest specific surface area. This is because that the flower-shaped nanostructure has the unique three-dimensional (3D) networks which can provide longer diffusion paths and the highest pore volume (0.66 cm^3 g^{-1}) which offers advantages in contact with and transport of the electrolyte.

Yu and coworkers [39] successfully prepared the three-dimensional (3D) network mesoporous nanostructured α-MnO_2 (MN-α-MnO_2) powders using an inexpensive glucose–permanganate sol–gel method at room temperature and under ambient pressure. The MN-α-MnO_2 exhibited high specific surface areas (ca. 220 m^2 g^{-1}) and narrow pore size distributions (5.6 nm) resulting in a good specific capacitance of 264 F g^{-1} after 1000 charge-discharge cycles.

3.4. Microwave-assisted method

Recently, microwave-assisted method has drawn large attention in the synthesis of oxide materials for supercapacitors application. Compared to conventional oil bath or hydrothermal heating, microwave heating can reduce the reaction time often by orders of magnitude, reduce the manufacturing cost and enhance product yield. An inverted temperature gradient takes place during the microwave-assisted process, and a rapid dielectric heating is generated internally within the material due to applied microwave radiation with a commonly used frequency of 0.3–2.45 GHz. Microwave-assisted synthesis has been adopted to prepare metal oxides with highly uniform nanostructures [40–42].

For example, Zhang et al. [43] have successfully synthesized γ-MnO_2 nanoparticles and α-MnO_2 urchin-like nanostructures by the microwave-assisted reflux as short as 5 min under neutral and acidic conditions, respectively. The γ-MnO_2 nanoparticles showed a smaller particle size, a higher specific surface area and a larger pore volume than those of α-MnO_2 urchin-like nanostructures resulting in a higher capacitance of 311 F g^{-1} at a current density of 0.2 A g^{-1}. The specific capacitance retention and coulombic efficiency after 5000 cycles at 1 A g^{-1} were about 93% and almost 100% for γ-MnO_2 nanoparticles, respectively.

Cao and coworkers [44] prepared flower-like NiO hollow nanosphere precursors via an efficient gas/liquid interfacial microwave-assisted process and were then transformed to NiO by simple calcinations. The wall of the sphere is composed of twisted NiO nanosheets that intercalated with each other. Such hollow structure is different from widely reported flower-like nanostructures with solid cores. These flower-like NiO hollow nanospheres have high surface area of 176 m^2 g^{-1}. Electrochemical properties show a high specific capacitance of 585 F g^{-1} at a discharge current of 5 A g^{-1} and excellent cycling stability.

3.5. Template-assisted method

Hard templates are those materials which are either used as scaffolds for the deposition or employed not only as shape defined templates, but also as chemical reagents that react with

other chemicals to produce desired nanomaterials. In the development of various metal oxide nanostructures, the hard template method is widely used and coupled with other methods, such as electrochemical deposition, solvothermal/hydrothermal and sol–gel methods. There are quite a lot of hard templates have been used for the synthesis of metal oxide nanostructures, such as porous anodic aluminum oxide (AAO), polycarbonate membranes (PC), carbon spheres, porous carbon, SiO_2 spheres, mesoporous silica and naturally existing diatomite.

The anodic aluminum oxide (AAO) film is also one of the attractive templates since it possesses very regular and highly anisotropic porous structures with pore diameters ranging from below 10 to 200 nm, pore length from 1 to 50 mm and pore densities in the range of 109–1011 cm^{-2} [45]. The pores have been found to be uniform and nearly parallel, which is useful for the synthesis of one-dimensional metal oxide nanostructures, affording short ion diffusion paths and fast kinetics during the electrochemical reactions. Using AAO as the template, Dar et al. [46] synthesized NiO nanotubes via electrochemical deposition and nanorods after 25 min annealing at 450°C. Due to a suitable combination of nanocrystalline grain size and the high surface area akin to the tubular structure, NiO nanotube exhibits an excellent supercapacitive performance with a maximum specific capacitance of 2093 F g^{-1} which approaches the theoretical value of NiO (2584 F g^{-1}). In contrast, the NiO nanorod structure is characterized by lower performance (797 F g^{-1}). Furthermore, both NiO nanotube and nanorod show high stabilities with almost no alteration to performance after 500 cycles at high current densities of 125 and 80 A g^{-1}. It has also been reported by Xu et al. [47] that Co_3O_4 nanotubes were successfully prepared via the AAO template method. The Co_3O_4 nanotubes have an average diameter of 300 nm and thickness of 50 nm which mainly controlled by the pore size of the AAO template. A good specific capacitance of 574 F g^{-1} was also obtained at a current density of 0.1 A g^{-1}. However, the high cost of AAO templates limits their large-scale application for the production of well-organized metal oxide nanostructured electrodes.

In addition to the AAO template, carbon-based materials with different structures were also developed to prepare metal oxides. For instance, Du et al. [26] reported that Co_3O_4 hollow spheres composed of numerous small nanocrystals were prepared via one-pot hydrothermal carbonization and calcination method with carbon spheres as templates. The specific capacitance is 470 F g^{-1} at a current density of 1 A g^{-1}, and no obvious capacitance decrease was observed over 1000 cycles of charge and discharge. Moreover, Yao et al. [48] synthesized nanostructured hierarchical mesoporous ribbon-like NiO via a hard-template method combining the calcination process. The mesoporous carbon was used as a hard template to control the structure growth and pore size distribution. A large surface area (147 m^2 g^{-1}) and high pore volume (0.2 cm^3 g^{-1}) were achieved when the molar ratio of Ni/C was 2/5. Notably, the outstanding pseudocapacitive performance was obtained with a high specific capacitance of 1260 F g^{-1} at a 1 A g^{-1} and only 5% deterioration of the initial capacitance after 5000 cycles.

4. Metal oxide-carbon composite electrodes

Preparing metal oxide-carbon composites is one of the most effective approaches to improve the supercapacitive performance of metal oxide electrodes. In such composite structures, the carbon materials with large specific surface area and high electric conductivity can provide the channels for charge transfer and benefit to the rate capability. Among a series of carbon materials, carbon nanotubes (CNTs), carbon nanofibers (CNFs), graphene and carbon nanofoams have been mostly studied to combine with metal oxide.

4.1. Metal oxide-carbon nanotubes (CNTs) composite

CNTs have outstanding pore structure, high electrical conductivity, and good mechanical and thermal stability which make them one of the most widely used carbon materials for supporting metal oxide. Thus, CNTs have been coupled with various metal oxides such as NiO, Co_3O_4, V_2O_5, MnO_2, SnO_2 and CuO to form the metal oxide–CNTs composite electrodes. It has been reported in 2005 that Lee et al. [49] synthesized NiO/CNTs nanocomposite via a hydrothermal method and explored the influences of CNT network existing in NiO. Compared to bare NiO, NiO/CNTs nanocomposite electrode exhibited a more rectangular shape in the CV curve and a smaller IR loss indicating a better supercapacitive performance. The specific capacitance increased from 122 to 160 F g^{-1} at a scan rate of 2 mV s^{-1} with the presence of 10% CNTs. The optimized properties owe to that CNTs can effectively improve the electrical conductivity of NiO and supply more active sites for redox reaction of NiO by increasing its specific surface area. After that, Lin et al. [50] prepared mesoporous sphere NiO nanostructures dispersing on the surface of CNTs and the maximum specific capacitance of 1329 F g^{-1} was observed at a very high current density of 84 A g^{-1}. Gund et al. [51] fabricated highly flexible electrode with NiO/MWCNTs nanohybrid thin films on stainless steel substrate with an excellent specific capacitance of 1727 F g^{-1} at a current density of 5 mA cm^{-2} and good stability (91% retention after 2000 cycles).

The advantages of the metal oxide-CNTs composite were further demonstrated. Cheng et al. synthesized nanocomposites of V_2O_5 nanowires and interpenetrating CNTs via a hydrothermal process. When the nanocomposite contained 33 wt% of the CNTs, the V_2O_5-CNTs showed the best specific capacitance of 530 F g^{-1} which was significantly higher than the V_2O_5 nanowires (146 F g^{-1}). The improved conductivity and the increased specific surface area (from 83 to 125 m^2 g^{-1}) were considered to be responsible for the better properties. Moreover, Wang et al. [52] designed a Co_3O_4@MWCNT nanocable using multiwall carbon nanotubes (MWCNTs) as the core cable. Compared to the pristine Co_3O_4 which has a low specific capacitance less than 130 F g^{-1}, the prepared Co_3O_4@MWCNT nanocable exhibits a better performance with a specific capacitance of 590 F g^{-1} at 15 A g^{-1} and 510 F g^{-1} even at 100 A g^{-1}. Furthermore, many efforts have been made on the preparation of MnO_2-CNTs nanocomposites in order to improve the supercapacitive performance of MnO_2. For example, MnO_2-CNTs composites were prepared through a modified one-pot reaction process by Li and coworkers [53]. This cross-linked MnO_2 nanoflakes-CNTs structure showed a good specific capacitance of 201 F g^{-1} and remarkable cycle stability (no obvious decay after

10,000 cycles). It has also been reported by Chen et al. [54] that MnO_2 nanoparticles were introduced into the inner wall of CNT channels by a wet-chemistry method. The result of electrochemical tests shows that the composite has a much higher specific capacitance of 225 F g^{-1} than MnO_2 with a value of 13 F g^{-1}.

4.2. Metal oxide-carbon nanofibers (CNFs) composite

CNFs are very attractive as the support for metal oxides in the composite electrodes due to their conductive networks with appropriate pore channels. Typically the metal oxides are coated on the CNFs surface to form a core–shell structure in which the CNFs can serves as the physical backbone support and offer the channel for efficient electron and ion transportation. Zhi and coworkers [55] reported the synthesis of CNFs/MnO_2 nano-composite with a coaxial cable structure as shown in **Figure 5a**. The CNFs with a diameter of 200 nm coated by 4-nm-thick MnO_2 nanowhiskers sheath giving a high specific surface area could be seen in **Figure 5b**. The nanocomposite electrode showed a good specific ca-pacitance of 311 F g^{-1} for the whole electrode and 900 F g^{-1} for the MnO_2 shell at a scan rate of 2 mV s^{-1}. In addition, **Figure 5c** and **d** indicated that this CNFs/MnO_2 nanocompo-site also exhibited good cycling stability (2.4% loss after 1000 cycles), high energy density (80.2 Wh kg^{-1}) and high power density (57.7 kW kg^{-1}). Moreover, a Fe_3O_4/CNFs nanocom-posite was designed by Fu et al. [56] through a solvent thermal reaction. Compared to the low specific capacitance (4 F g^{-1}) of pure Fe_3O_4, the calculated specific capacitance of Fe_3O_4/CNFs nanocomposite is as high as 127 F g^{-1} which indicates a better supercapacitive per-formance. The CNFs have not only improved the electronic/ionic conductivity of Fe_3O_4, but also prevented the aggregation of Fe_3O_4 nanosheets. CuO has also been used to fabri-cate composite with CNFs in order to improve its supercapacitive performance. As report-ed by Moosavifard [57], one-dimensional hierarchical hybrid CuO nanorod arrays-CNFs composite has been prepared via a solution method and an annealing treatment. The CuO nanorods with a length of around 300 nm and a diameter of around 15 nm are grown uniformly surrounding the CNFs. It should be noted that empty space existed among ad-jacent nanorods indicating a hierarchical array structure. The unique nanocomposite struc-ture contributed to a high capacitance of 398 F g^{-1}.

In addition, carbon fibers can also form a paper. Ghosh et al. [58] prepared carbon nanofiber paper (CFP) with fiber diameters ranging from 100 to 300 nm by electrospinning the polya-crylonitrile (PAN) precursor. The CFP showed good conductivity (0.1 S cm^{-1}), high porosity and large surface area of 700 m^2 g^{-1} indicating its potential to be a promising material for supporting metal oxide. Using this carbon nanofiber paper as substrate, 3-nm-thick V_2O_5 was obtained by electrodeposition method. The V_2O_5-CFP composite exhibited a total specific capacitance of 214 F g^{-1}. Recently, Yang et al. [59] have reported a CFP/Co_3O_4 paper electrode with an excellent specific capacitance of 1124 F g^{-1} at a high current density of 25.34 A g^{-1} in the NaOH electrolyte. The composite also displayed a remarkable electrochemical stability with around 94.4% retention after 5000 charge-discharge cycles. The outstanding supercapa-citive performance was attributed to the unique 1D nanonet structure of the electrodes and the improved electronic conductivity as well as ion diffusion by CFP.

4.3. Metal oxide-graphene composite

Since a mechanically exfoliated graphene monolayer was first observed and characterized in 2004, considerable research has been carried out in supercapacitor applications due to its large theoretical specific area (2630 m^2 g^{-1}), high electrical conductivity (104 S cm^{-2}), abundant raw material resource and good electrochemical stability [60]. Therefore, graphene with these fascinating properties is expected as the potential supporting materials to improve the performance of metal oxide-based supercapcitors. Besides graphene, graphene oxide (GO) and reduced graphene oxide (rGO) have also attracted considerable attention due their unique physical and chemical properties. Until now, various metal oxides such as NiO, MnO_2, CuO, V_2O_5, Co_3O_4 and TiO_2 have been coupled with graphene materials to form supercapacitor electrodes for superior performance.
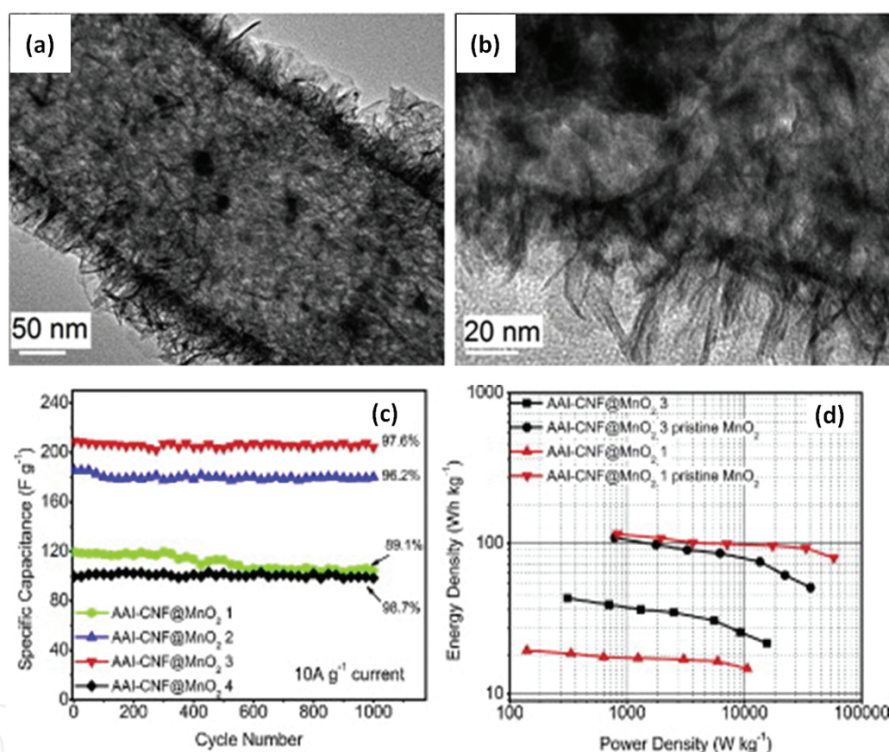

Figure 5. (a) TEM images of a single CNF@MnO_2 nanostructure and (b) the MnO_2 porous shell with nanowhiskers; (c) stability of the CNF@MnO_2 electrodes; (d) Ragone plots of the CNF@MnO_2 electrodes [55].

For example, Ge et al. [61] reported the preparation of 3D flower-like NiO and graphene sheets composite via incorporating a facile hydrothermal process with a thermal treatment process. The resultant composite exhibits a specific capacitance of 346 F g^{-1} (1.5 A g^{-1}), a good rate performance and cycle stability in 2 M KOH. It should be noted that NiO in the composite could provide a specific capacitance as high as 778.7 F g^{-1}, which far exceeded the bare NiO of only 220 F g^{-1}. The magnitude of equivalent series resistances (ESR) are 0.71, 0.99 and 0.85 Ω cm^{-2} for graphene sheet, NiO and composite, respectively, indicating that the conductivity of the composite is improved by the presence of graphene sheets

which could contribute to the superior supercapacitive performance of NiO. Wu et al. [62] successfully synthesized NiO particles/graphene oxide (GO) nanosheets composites. Compared with pure NiO and graphene, the composite electrode showed highest current response during CV scanning, reflecting the high capacitance value. The specific capacitance of the NiO/GO composite electrode (460 F g^{-1}) is much higher than those of the bare graphene oxide electrode (13 F g^{-1}) and NiO (40 F g^{-1}) electrode at a current density of 10 A g^{-1}. In addition, the capacitance retention of NiO/GO composite can remain nearly 100% after 3000 cycles which indicates excellent cycle-life stability. Moreover, Co_3O_4/graphene nanosheet (GNS) composite has been synthesized via a microwave-assisted method by Yan et al. [63]. The Co_3O_4 nanoparticles with a small size of 3–5 nm were uniformly distributed on the surface of graphene sheets. The electrochemical properties of composite were observed with a good specific capacitance of 243.2 F g^{-1} and an outstanding stability (only 4.3% loss after 2000 cycles).

Recently, the uniform rod-like V_2O_5 nanocrystals have been fabricated on the surface of reduced graphene oxide (rGO) to form the V_2O_5-rGO nanocomposites as the supercapacitor electrode [64]. The V_2O_5 nanoparticles on rGO were prepared by hydrolysing vanadium oxytripropoxide (VOTP) in ethanol solution with the existence of GO. For a comparative study, the pure V_2O_5 was also prepared in the same condition but without GO. The results have shown that the electrochemical performance of the V_2O_5-rGO nanocomposites with an excellent specific capacitance of 537 F g^{-1} at a current density of 1 A g^{-1} was much better than pure V_2O_5 which had a relatively low value of 202 F g^{-1}. After 1000 charge-discharge cycles, the composite electrode could retain 84% of its initial capacitance while only 30% was retained for pure V_2O_5 indicating that V_2O_5-rGO nanocomposite electrode had a better electrochemical stability. In addition, the higher power and energy densities were also obtained in the composite. The synergistic effect of V_2O_5 nanorods and rGO has been considered to be responsible for the better supercapacitive performance. Firstly, the conductivity can be improved due to the presence of rGO. Secondly, the nanocomposites possess a larger surface area (49.16 m^2 g^{-1}) than that of pure V_2O_5 (37.57 m^2 g^{-1}). Thirdly, the rGO sheets can inhibit the disintegration of V_2O_5 and buffer the strain aroused by the volume expansion during the charging and discharging processes. Finally, the strong adhesion between V_2O_5 nanorods and rGO sheets may facilitate fast electron transfer through the highly conductive rGO sheets. Similarly, Xiang et al. [65] fabricated the rGO–TiO_2 nanobelt composite by a hydrothermal processing in the ethanol solution. When the rGO/TiO_2 mass ratio was 7:3, the composite obtained the best specific capacitance of 200 F g^{-1} which far exceeded pure TiO_2 nanobelt (17 F g^{-1}) and rGO (40 F g^{-1}) in the Na_2SO_4 electrolyte at a scan rate of 2 mV s^{-1}.

4.4. Metal oxide-carbon foams composite

In addition to high specific capacitance, high energy density and power density are also desirable for metal oxide-based supercapacitors. In general, increasing the mass loading can effectively store more energy and power. However, it is a challenge to load a large amount of materials on electrode without undermining the electrochemical performance. One promising

approach is to form metal oxide-carbon nanofoams composite as electrodes. Three-dimensional (3D) carbon nanofoams with a through-connected pore network possess large specific surface areas allowing high metal oxide loading. Moreover, the high electric conductivity of carbon nanofoams can improve the electrochemical properties of metal oxide. Chen et al. [66] fabricated nanostructured MnO_2 on CNT foams (or sponges) and the flower-like MnO_2 nanoparticles were uniformly deposited on the skeleton of CNT sponges. An outstanding specific capacitance of 1270 F g^{-1} close to the theoretical value has been obtained and only 4% of degradation after 10,000 cycles at a charge-discharge current density of 5 A g^{-1}. Furthermore, the specific power and energy of this composite are high with values of 63 kW kg^{-1} and 31 Wh kg^{-1}, respectively. Dong and co-workers deposited Co_3O_4 nanowires on the 3D graphene foam in [67]. It can be seen in the figure, the graphene skeleton is fully and uniformly covered by the network of Co_3O_4 nanowires together provide a large accessible surface area. The composite electrode exhibited a high specific capacitance of ~1100 F g^{-1} after 500 cycles at a current density of 10 A g^{-1} and stayed stable afterward indicating a good cycling stability.

5. Conclusion

This chapter presents a relatively general understanding of the correlation between the composition, microstructure and electrochemical behaviors of metal oxide nanostructures-based electrodes for the applications of supercapacitors. The current possibility of controlled growth and self-assembly represents an important step toward the design and tuning of metal oxide nanocrystals, and also it will be a significant step to the applications of metal oxides as ideal electrodes in high performance electrochemical energy storage devices.

Author details

Zhenjun Qi[*], Shihao Huang, Adnan Younis, Dewei Chu and Sean Li

*Address all correspondence to: zhenjun.qi@student.unsw.edu.au

School of Materials Science and Engineering, University of New South Wales, Sydney, NSW, Australia

References

[1] Conway, B.E., Transition from "supercapacitor" to "battery" behavior in electrochemical energy storage. Journal of the Electrochemical Society, 1991. 138(6): p. 1539–1548.

[2] Kandalkar, S., et al., Chemical synthesis of cobalt oxide thin film electrode for supercapacitor application. Synthetic Metals, 2010. 160(11): p. 1299–1302.

[3] Zhang, L.L. and X. Zhao, Carbon-based materials as supercapacitor electrodes. Chemical Society Reviews, 2009. 38(9): p. 2520–2531.

[4] Simon, P. and Y. Gogotsi, Materials for electrochemical capacitors. Nature Materials, 2008. 7(11): p. 845–854.

[5] Jayalakshmi, M. and K. Balasubramanian, Simple capacitors to supercapacitors-an overview. International Journal of Electrochemical Science, 2008. 3(11): p. 1196–1217.

[6] Padhi, A.K., K. Nanjundaswamy, and J. Goodenough, Phospho-olivines as positive-electrode materials for rechargeable lithium batteries. Journal of the Electrochemical Society, 1997. 144(4): p. 1188–1194.

[7] Kötz, R. and M. Carlen, Principles and applications of electrochemical capacitors. Electrochimica Acta, 2000. 45(15): p. 2483–2498.

[8] Zhang, S. and G.Z. Chen, Manganese oxide based materials for supercapacitors. Energy Materials, 2008. 3(3): p. 186–200.

[9] Sharma, P. and T. Bhatti, A review on electrochemical double-layer capacitors. Energy Conversion and Management, 2010. 51(12): p. 2901–2912.

[10] Babakhani, B. and D.G. Ivey, Improved capacitive behavior of electrochemically synthesized Mn oxide/PEDOT electrodes utilized as electrochemical capacitors. Electrochimica Acta, 2010. 55(12): p. 4014–4024.

[11] Huang, M., et al., MnO_2-based nanostructures for high-performance supercapacitors. Journal of Materials Chemistry A, 2015. 3(43): p. 21380–21423.

[12] Burke, A., Ultracapacitors: why, how, and where is the technology. Journal of Power Sources, 2000. 91(1): p. 37–50.

[13] Vangari, M., T. Pryor, and L. Jiang, Supercapacitors: review of materials and fabrication methods. Journal of Energy Engineering, 2012. 139(2): p. 72–79.

[14] Conway, B.E., Electrochemical capacitors based on pseudocapacitance. In: Electrochemical Supercapacitors. Springer US; 1999. p. 221–257.

[15] Zhi, M., et al., Nanostructured carbon–metal oxide composite electrodes for supercapacitors: a review. Nanoscale, 2013. 5(1): p. 72–88.

[16] Zheng, J., P. Cygan, and T. Jow, Hydrous ruthenium oxide as an electrode material for electrochemical capacitors. Journal of the Electrochemical Society, 1995. 142(8): p. 2699–2703.

[17] Wei, J., N. Nagarajan, and I. Zhitomirsky, Manganese oxide films for electrochemical supercapacitors. Journal of Materials Processing Technology, 2007. 186(1): p. 356–361.

[18] Devaraj, S. and N. Munichandraiah, Effect of crystallographic structure of MnO_2 on its electrochemical capacitance properties. The Journal of Physical Chemistry C, 2008. 112(11): p. 4406–4417.

[19] Brock, S.L., et al., A review of porous manganese oxide materials. Chemistry of Materials, 1998. 10(10): p. 2619–2628.

[20] Brousse, T., et al., Crystalline MnO_2 as possible alternatives to amorphous compounds in electrochemical supercapacitors. Journal of the Electrochemical Society, 2006. 153(12): p. A2171-A2180.

[21] Wang, G., L. Zhang, and J. Zhang, A review of electrode materials for electrochemical supercapacitors. Chemical Society Reviews, 2012. 41(2): p. 797–828.

[22] Gao, Y., et al., Electrochemical capacitance of Co_3O_4 nanowire arrays supported on nickel foam. Journal of Power Sources, 2010. 195(6): p. 1757–1760.

[23] Lu, Z., et al., Stable ultrahigh specific capacitance of NiO nanorod arrays. Nano Research, 2011. 4(7): p. 658–665.

[24] Huang, M., et al., Self-assembly of mesoporous nanotubes assembled from interwoven ultrathin birnessite-type MnO_2 nanosheets for asymmetric supercapacitors. Scientific Reports, 2014. 4: p. 3878.

[25] Yan, X., et al., Rational synthesis of hierarchically porous NiO hollow spheres and their supercapacitor application. Materials Letters, 2013. 95: p. 1–4.

[26] Du, H., et al., Facile carbonaceous microsphere templated synthesis of Co_3O_4 hollow spheres and their electrochemical performance in supercapacitors. Nano Research, 2013. 6(2): p. 87–98.

[27] Moosavifard, S.E., et al., Designing 3D highly ordered nanoporous CuO electrodes for high-performance asymmetric supercapacitors. ACS Applied Materials & Interfaces, 2015. 7(8): p. 4851–4860.

[28] Wang, Y., et al., Synthesis of 3D-nanonet hollow structured Co_3O_4 for high capacity supercapacitor. ACS Applied Materials & Interfaces, 2014. 6(9): p. 6739–6747.

[29] Qi, Z., et al., A facile and template-free one-pot synthesis of Mn_3O_4 nanostructures as electrochemical supercapacitors. Nano-Micro Letters, 2016. 8(2): p. 165–173.

[30] Nandy, S., et al., Enhanced p-type conductivity and band gap narrowing in heavily Al doped NiO thin films deposited by RF magnetron sputtering. Journal of Physics: Condensed Matter, 2009. 21(11): p. 115804.

[31] Hamdani, M., R. Singh, and P. Chartier, Co_3O_4 and Co-based spinel oxides bifunctional oxygen electrodes. International Journal of Electrochemical Science, 2010. 5(4): p. 556.

[32] Yang, J., et al., Nanostructured porous MnO$_2$ on Ni foam substrate with a high mass loading via a CV electrodeposition route for supercapacitor application. Electrochimica Acta, 2014. 136: p. 189–194.

[33] Purushothaman, K.K., et al., Nanosheet-assembled NiO microstructures for high-performance supercapacitors. ACS Applied Materials & Interfaces, 2013. 5(21): p. 10767–10773.

[34] Xia, X.-h., et al., Self-supported hydrothermal synthesized hollow Co$_3$O$_4$ nanowire arrays with high supercapacitor capacitance. Journal of Materials Chemistry, 2011. 21(25): p. 9319–9325.

[35] Aghazadeh, M., et al., A facile route to preparation of Co$_3$O$_4$ nanoplates and investigation of their charge storage ability as electrode material for supercapacitors. Journal of Materials Science: Materials in Electronics, 2016. 27(8) p. 1–10.

[36] Deng, M.-J., et al., Facile electrochemical synthesis of 3D nano-architectured CuO electrodes for high-performance supercapacitors. Journal of Materials Chemistry A, 2014. 2(32): p. 12857–12865.

[37] Lee, S.H., et al., Morphology and composition control of manganese oxide by the pulse reverse electrodeposition technique for high performance supercapacitors. Journal of Materials Chemistry A, 2013. 1(46): p. 14606–14611.

[38] Kim, S.-I., et al., Facile route to an efficient NiO supercapacitor with a three-dimensional nanonetwork morphology. ACS Applied Materials & Interfaces, 2013. 5(5): p. 1596–1603.

[39] Yu, L.L., J.J. Zhu, and J.T. Zhao, Three-dimensional network mesoporous nanostructured α-manganese dioxide with high supercapacitive performance: facile, environmental and large-scale synthesis. European Journal of Inorganic Chemistry, 2013. 2013(21): p. 3719–3725.

[40] Bilecka, I. and M. Niederberger, Microwave chemistry for inorganic nanomaterials synthesis. Nanoscale, 2010. 2(8): p. 1358–1374.

[41] Truong, T.T., et al., Morphological and crystalline evolution of nanostructured MnO$_2$ and its application in lithium–air batteries. ACS Nano, 2012. 6(9): p. 8067–8077.

[42] Pahalagedara, L., et al., Microwave-assisted hydrothermal synthesis of α-MnO$_2$: lattice expansion via rapid temperature ramping and framework substitution. The Journal of Physical Chemistry C, 2014. 118(35): p. 20363–20373.

[43] Zhang, X., et al., Microwave-assisted reflux rapid synthesis of MnO$_2$ nanostructures and their application in supercapacitors. Electrochimica Acta, 2013. 87: p. 637–644.

[44] Cao, C.-Y., et al., Microwave-assisted gas/liquid interfacial synthesis of flowerlike NiO hollow nanosphere precursors and their application as supercapacitor electrodes. Journal of Materials Chemistry, 2011. 21(9): p. 3204–3209.

[45] Liu, N.W., et al., Fabrication of anodic-alumina films with custom-designed arrays of nanochannels. Advanced Materials, 2005. 17(2): p. 222–225.

[46] Dar, F.I., K.R. Moonoosawmy, and M. Es-Souni, Morphology and property control of NiO nanostructures for supercapacitor applications. Nanoscale Research Letters, 2013. 8(1): p. 1.

[47] Xu, J., et al., Preparation and electrochemical capacitance of cobalt oxide (Co_3O_4) nanotubes as supercapacitor material. Electrochimica Acta, 2010. 56(2): p. 732–736.

[48] Yao, M., et al., Template synthesis and characterization of nanostructured hierarchical mesoporous ribbon-like NiO as high performance electrode material for supercapacitor. Electrochimica Acta, 2015. 158: p. 96–104.

[49] Lee, J.Y., et al., Nickel oxide/carbon nanotubes nanocomposite for electrochemical capacitance. Synthetic Metals, 2005. 150(2): p. 153–157.

[50] Lin, P., et al., The nickel oxide/CNT composites with high capacitance for supercapacitor. Journal of the Electrochemical Society, 2010. 157(7): p. A818-A823.

[51] Gund, G.S., et al., Architectured morphologies of chemically prepared NiO/MWCNTs nanohybrid thin films for high performance supercapacitors. ACS Applied Materials & Interfaces, 2014. 6(5): p. 3176–3188.

[52] Wang, X., et al., Co_3O_4@ MWCNT nanocable as cathode with superior electrochemical performance for supercapacitors. ACS Applied Materials & Interfaces, 2015. 7(4): p. 2280–2285.

[53] Li, L., et al., Facile synthesis of MnO_2/CNTs composite for supercapacitor electrodes with long cycle stability. The Journal of Physical Chemistry C, 2014. 118(40): p. 22865–22872.

[54] Chen, W., et al., Enhanced capacitance of manganese oxide via confinement inside carbon nanotubes. Chemical Communications, 2010. 46(22): p. 3905–3907.

[55] Zhi, M., et al., Highly conductive electrospun carbon nanofiber/MnO_2 coaxial nanocables for high energy and power density supercapacitors. Journal of Power Sources, 2012. 208: p. 345–353.

[56] Fu, C., A. Mahadevegowda, and P.S. Grant, Fe_3O_4/carbon nanofibres with necklace architecture for enhanced electrochemical energy storage. Journal of Materials Chemistry A, 2015. 3(27): p. 14245–14253.

[57] Moosavifard, S.E., et al., Facile synthesis of hierarchical CuO nanorod arrays on carbon nanofibers for high-performance supercapacitors. Ceramics International, 2014. 40(10): p. 15973–15979.

[58] Ghosh, A., et al., High pseudocapacitance from ultrathin V_2O_5 films electrodeposited on self-standing carbon-nanofiber paper. Advanced Functional Materials, 2011. 21(13): p. 2541–2547.

[59] Yang, L., et al., Hierarchical network architectures of carbon fiber paper supported cobalt oxide nanonet for high-capacity pseudocapacitors. Nano Letters, 2011. 12(1): p. 321–325.

[60] Stoller, M.D., et al., Graphene-based ultracapacitors. Nano Letters, 2008. 8(10): p. 3498–3502.

[61] Ge, C., et al., Three-dimensional flower-like nickel oxide supported on graphene sheets as electrode material for supercapacitors. Journal of Sol-Gel Science and Technology, 2012. 63(1): p. 146–152.

[62] Wu, M.-S., et al., Formation of nano-scaled crevices and spacers in NiO-attached graphene oxide nanosheets for supercapacitors. Journal of Materials Chemistry, 2012. 22(6): p. 2442–2448.

[63] Yan, J., et al., Rapid microwave-assisted synthesis of graphene nanosheet/Co_3O_4 composite for supercapacitors. Electrochimica Acta, 2010. 55(23): p. 6973–6978.

[64] Li, M., et al., Controlling the formation of rodlike V_2O_5 nanocrystals on reduced graphene oxide for high-performance supercapacitors. ACS Applied Materials & Interfaces, 2013. 5(21): p. 11462–11470.

[65] Xiang, C., et al., Reduced graphene oxide/titanium dioxide composites for supercapacitor electrodes: shape and coupling effects. Journal of Materials Chemistry, 2012. 22(36): p. 19161–19167.

[66] Chen, W., et al., High-performance nanostructured supercapacitors on a sponge. Nano Letters, 2011. 11(12): p. 5165–5172.

[67] Dong, X.-C., et al., 3D graphene–cobalt oxide electrode for high-performance supercapacitor and enzymeless glucose detection. ACS Nano, 2012. 6(4): p. 3206–3213.